NCEE Working Paper

Monetizing the impacts of ocean warming and acidification on shellfisheries of the United States and Canada

Chris Moore, Travis Tai, Corinne Hartin, and Stephen R. Pacella

Working Paper 24-03
June, 2024

U.S. Environmental Protection Agency
National Center for Environmental Economics
https://www.epa.gov/environmental-economics

NCEE
NATIONAL CENTER FOR ENVIRONMENTAL ECONOMICS

Monetizing the impacts of ocean warming and acidification on shellfisheries of the United States and Canada

Chris Moore, U.S. EPA, National Center for Environmental Economics

Travis Tai, Pacific Biological Station, Fisheries and Oceans Canada

Corinne Hartin, U.S. EPA, Office of Air and Radiation Climate Change Division

Stephen R. Pacella, US EPA, Office of Research and Development, Center for Public Health and Environmental Assessment

Abstract

Anthropogenic greenhouse gas emissions are driving changes in marine environments and affecting marine fisheries. In the coming decades, ocean warming and acidification will cause changes in the habitable range and stocks of commercially valuable shellfish species. This study estimates the monetary impacts to shellfish consumers in the US and Canada using an inverse demand and consumer welfare model. Taking harvest forecasts for 17 types of shellfish under two greenhouse gas emissions scenarios through the end of this century, we model consumer substitution patterns, changes in expenditures, and annual welfare impacts in shellfish markets. Finally, we use the welfare results to estimate a reduced form damage function that can be used in existing integrated assessment models for climate policy analysis. We find that US consumers experience damages far greater than Canadian consumers due to the relative size of the markets in each country and differences in habitat suitability as waters off the coasts of both countries become warmer and more acidic. The net present value of impacts through 2100 to US consumers is about $11.3 billion USD and $850 million USD for Canadian consumers. Our model results also allow us to monetize the impacts of warming and acidification separately, showing that most of the consumer welfare impacts are attributable to warming and a small fraction of total damages can be attributed to acidification.

Keywords: Economic impacts, climate change, ocean acidification, commercial fishing

JEL Codes: Q54, Q22

Disclaimer: The findings, conclusions, and views expressed here are those of the authors alone and do not necessarily reflect those of the United States Environmental Protection Agency. No official Agency endorsement has been granted, nor should such endorsement be inferred.

Introduction

Anthropogenic greenhouse gas (GHG) emissions negatively impact marine species in two distinct ways. The warming of the oceans caused by climate change is impacting the availability of suitable habitat for some commercially valuable species (Pinsky et al. 2018). In addition to the temperature driven impacts of climate change, carbon dioxide (CO_2) emissions are acidifying ocean waters and affecting the ability of marine calcifiers to build shells and skeletal structures (Doney et al. 2020). This understanding of the biological and ecological impacts of ocean acidification (OA) and climate change has resulted from focused experimental and observational research over the past two decades (e.g., Kroeker et al. 2013; Bednaršek et al. 2021), and recent studies have begun to leverage this knowledge of taxon-specific effects to forecast population-level impacts of future climate change over broad spatial scales (e.g., Tai, Sumaila, and Cheung 2021; Doney et al. 2020 and references therein). In parallel, the societal and economic impacts of OA have been characterized through vulnerability assessments (e.g., Ekstrom et al. 2015; Berger 2022) and economic forecasting studies (Moore and Fuller 2022 and references therein). Projecting the societal impacts of climate change on fisheries has been a recent focus of study, including the impacts of ocean acidification on US (Cooley and Doney 2009; Moore et al. 2021) and global shellfisheries (Narita, Rehdanz, and Tol 2012).

The marine impacts of GHG emissions are not currently captured by national or global-scale valuations of climate change impacts commonly used by policymakers, such as the social cost of carbon dioxide and other GHGs (U.S. EPA 2022). The omission of marine impacts potentially underestimates the economic damages of climate change and including them has been highlighted as a research priority by policy analysts (Rennert et al. 2022). Addressing this omission requires an understanding of the relationship between GHG emissions and the monetized social impacts on marine resources such as stocks of fish and shellfish and the integrity of coral reefs. There is a growing number of studies that estimate the monetary impacts of climate change and OA on marine resources, but none has estimated the functional relationships necessary to forecast marginal economic impacts in a particular year under any given GHG emissions scenario. Most of the studies that estimate the economic impacts of climate change and OA on marine resources focus on shellfish (Moore 2015; Ekstrom et al. 2015; Narita and Rehdanz 2017), while others forecast impacts to finfish markets (Speers et al. 2016; Moore et al. 2021), and ecosystem services provided by coral reefs (Brander et al. 2012). While these studies make important advances in integrated modeling by linking global circulation models, biophysical impacts, and economic analyses, they do not provide the results required to estimate the general and reduced form functional relationships used by policy makers.

This study provides such results for impacts to shellfisheries of US and Canada. We do so by utilizing results from a recent study on climate change and OA impacts to global shellfish harvest (Tai, Sumaila, and Cheung 2021) as inputs to a model of consumer demand and welfare. Our approach considers the impacts of changing pH and ocean temperature on 17 shellfish species important to US and Canadian wild capture fisheries under a stringent global mitigation scenario and a high emissions scenario through 2100. Our focus on the United States and Canada demonstrates how climate change and OA can create “winners” and “losers” between marine jurisdictions via spatial heterogeneity in the impacts on marine resources. While our model does not take aquaculture and the implied mitigation possibilities into consideration, that omission is unlikely to have a substantial impact on our results. In the US, aquaculture accounted for about 10% of the value of shellfish harvest since 2011 and in Canada it was less than 5%. Further, only a fraction of a cultured mollusk’s life is spent in a controlled

environment. Most of their lives are spent in the open water where they are subject to the same ambient conditions as wild harvest that we model in this paper.

Data and Methods

This study takes a multidisciplinary approach to model the consumer welfare impacts of climate change and OA on wild shellfish harvests. Outputs from a dynamic bioclimatic model (Tai, Sumaila, and Cheung 2021) provide forecasted changes in the maximum harvest potential for shellfish in each year through 2100[1]. A consumer demand and welfare model provides annual economic impacts from the forecasted changes in harvests. Finally, the annual impacts and global mean temperature serve as datapoints to estimate a reduced form damage function that is consistent with current social cost of greenhouse gases estimation approaches (U.S. EPA 2022).

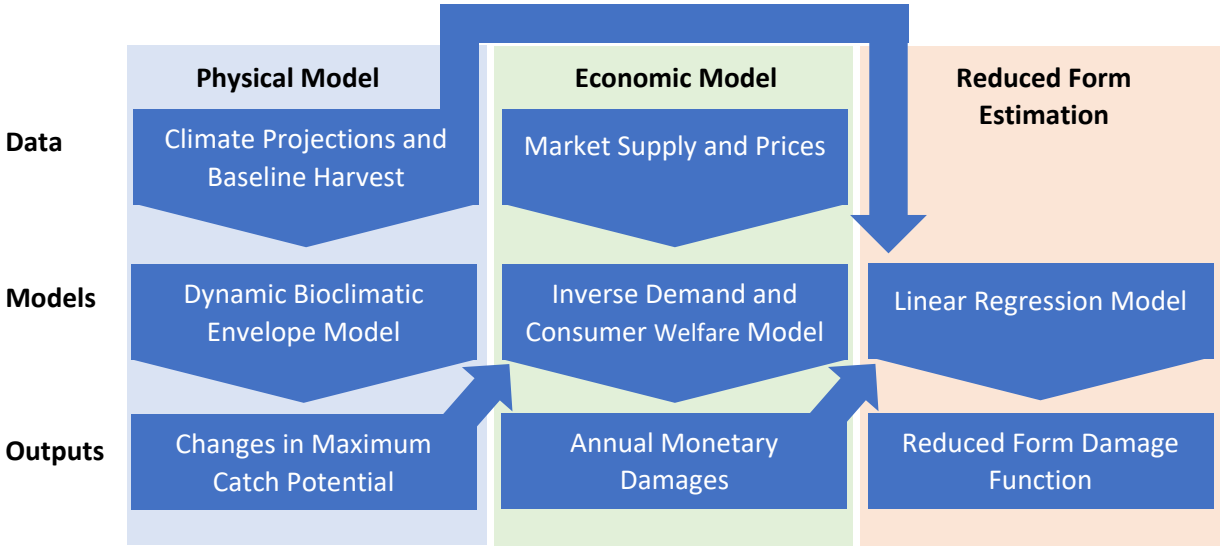

Figure 1. A schematic flowchart of the modeling approach beginning with climate projections and baseline harvest data used as inputs to the dynamic bioclimatic model, followed by the consumer demand and welfare model, and finally, reduced form estimation of the damage function.

Dynamic Bioclimate Envelope Model

The dynamic bioclimate envelope model (DBEM) (Cheung, Lam, and Pauly 2008; Cheung et al. 2011) is a spatially explicit model that projects changes in species' populations using a combination of empirical observations and structural equations. Changes in environmental conditions (e.g., temperature, salinity, primary production) affect the habitat suitability for each species, and, in turn, the population distribution and abundance, which can then be used to estimate and compare changes in future fisheries catch across marine regions. The DBEM integrates a combination of growth, ecophysiological, advection-diffusion, and surplus production population models to predict how changes in environmental

[1] While climate impacts are expected to last beyond 2100 under most scenarios, the damage function we estimate in this paper is invariant with respect to time so extrapolation beyond 2100 is not constrained by the time horizon of the DBEM.

conditions affect species populations. We summarize pertinent aspects of the model here, see Tai et al. (2021) for details.

The model forecasts changes in species biomass, *B,* over time using a derived von Bertalanffy model (Cheung et al. 2011; Pauly and Cheung 2018; Tai, Harley, and Cheung 2018) that is a function of changes in ocean temperature, oxygen content, and pH. Additionally, we model physiological changes in growth as a function of body weight *W,* such that:

$$\frac{dB}{dt} = H_{i,t}W^d - k_{i,t}W, \quad (1)$$

where *H* and *k* represent the coefficients for oxygen supply (anabolism) and oxygen demand for maintenance metabolism (catabolism), respectively, for grid cell *i* at time *t*. *H* is a function of ocean temperature and dissolved oxygen levels, and *k* is a function of ocean temperature and hydrogen ion concentration such that (see SI equations S.2 and S.3). The exponent *d* generally falls between 0.5 and 0.95 for invertebrates and we set it equal to 0.7 for this simulation. Anabolic processes scale linearly with dissolved oxygen concentration, while catabolic processes scale linearly with hydrogen concentration (lowering of pH). Both anabolic and catabolic processes scale to the root with temperature following the Arhennius equation (equations S.2 and S.3 in the Supplementary Material). The environmentally driven changes in *H* and *k* result in changes to maximum and mean body size of individuals within the population, which subsequently affect population parameters such as mortality (Pauly 1980, equations S6 to S9 in the Supplementary Material).

A logistic growth model captures population dynamics through species abundance, *A*,

$$A_{i,t+1} = A_{i,t} + rA_{i,t}\left(1 - \frac{A_{i,t}}{C_{i,t}}\right) + \sum_{j=1}^{N}\left(L_{j,i,t} + I_{j,i,t}\right) - A_{i,t}\left(1 - e^{-(F_{i,t}+M_{i,t})}\right) \quad (2)$$

where A is species abundance, *r* is the intrinsic population growth rate of the species, $C_{i,t}$ is the carrying capacity for each cell *i*, $L_{j,i,t}$ and $I_{j,i,t}$ are the settled larvae and net migrated adults, respectively, into cell *i* from surrounding cells *j*, $F_{i,t}$ is the fishing mortality rate, and *M* is the natural mortality rate (estimated from equation S10). Maximum sustainable yield (MSY) is the theoretical maximum biomass that can be sustainably removed from the population indefinitely. Maximum sustainable yield and the fishing mortality rate at MSY (F_{MSY}) are calculated using a Gordon Schaefer population growth model (Walters and Martell 2004), such that $MSY = \frac{B_\infty \cdot r}{4}$ and $F_{MSY,i,t} = \frac{r}{2}$, where B_∞ is the population carrying capacity. The US Magnuson–Stevens Fishery Conservation and Management Act and several United Nations Food and Agriculture Organization agreements and guidelines use the concept of MSY to set upper limits on sustainable harvest (Mace 2001). As such, we use MSY as a proxy for the maximum catch potential (MCP) for each of the fishery stocks analyzed in this model.

Initial Conditions and Climate Forecasts

Initial species distributions for 17 shellfish species were obtained using the approach of Palomares et al. (2016), for which a rule-based algorithm was applied to include a series of geographical constraints: latitudinal range, depth range, occurring ocean basins, and published or expert-provided bounding box for distribution range. The distributions are mapped on a global 0.5˚ longitude by 0.5˚ latitude grid, and matched to historical reconstructed catch data (www.seaaroundus.org) (Pauly and Zeller 2015) assumed to be distributed accordingly with relative abundance (Cheung, Lam, and Pauly 2008). Input data of

historical climatological data and species-specific parameters were used to generate the initial conditions and environmental preferences of species populations (1971-2000 average).

The model uses ocean outputs of sea surface temperature, chemistry, and O_2 from three CMIP5 Earth system models[2] under two future projections, RCP 2.6 and RCP 8.5 (Bopp et al. 2013). The RCP 2.6 scenario corresponds to a low climate change scenario that assumes immediate mitigation of GHG emissions where annual emissions peak by 2025. The RCP 8.5 scenario corresponds to a high climate change scenario in which emissions continue to increase through the end of the century. The three Earth system models provide sea surface and bottom layers and the full range of environmental variables required by the DBEM for both RCP scenarios (Cheung, Reygondeau, and Frölicher 2016).

Consumer Demand and Welfare Model

The purpose of the economic model is to use the forecasted changes in shellfish harvests to estimate consumer welfare impacts under the modeled climate change scenarios. To do so, a system of demand equations is derived from a model of consumer utility. We then use historical price and quantity data to estimate the parameters of the demand system. Next, we derive an expression for the monetary compensation consumers would require to achieve a reference level of utility when facing different supplies of shellfish. Finally, that expression is evaluated using estimated demand parameters and forecasted changes in harvest to solve for annual consumer welfare impacts through the end of the century.

A Two-Stage Inverse Demand System

Demand systems are usually estimated by holding either price or quantity fixed and solving for the free variable that would clear the market. In the case of fish, shellfish, and many agricultural products, the supplies of the commodities are held fixed, and price adjusts to clear the market (Barten and Bettendorf 1989; Park, Thurman, and Easley 2004). This approach recognizes that production decisions are usually made before producers can observe consumer demand and the perishability of the commodity prevents producers from adjusting supply in the short run to respond to market conditions.

The number of shellfish types that we model here makes the estimation of a single system with a demand equation for each type intractable. Instead, we take a two-stage budgeting approach to circumvent this dimensionality problem (Edgerton 1997). Under a two-stage budgeting approach, consumers first allocate their income among groups of commodities consisting of closely related goods. In a second stage of budget allocation, consumers divide each subset of their income among the individual commodities. This approach places some reasonable restrictions on the substitution patterns between goods but simplifies estimation immensely.

The functional form we use to estimate the welfare parameters is known as the inverse almost ideal demand system (Deaton and Muellbauer 1980) and can be represented using expenditure shares, S, where $S_f = \frac{X_f P_f}{Y}$, where X_f is the quantity of good f, P_f is its price, and Y is total expenditures on goods in the system. When estimating the first stage, X_f refers to aggregated quantities for goods in commodity group f and P_f is the average unit price in that group. When estimating the second stage, we estimate a system for each group and X_f are the landings for shellfish f and P_f are shellfish-specific prices.

[2] NOAA's Geophysical Fluid Dynamics Laboratory (GFDL-ESM), Institute Pierre Simon Laplace Climate Modelling Centre (IPSL-ESM), and Max Planck Institute for Meteorology (MPI-ESM)

The parameters of the expenditure share equations in each stage are found using the following system of estimating equations,

$$S_f = \alpha_f + \sum_f \gamma_{fg} \ln(X_g) - \beta_f lnQ, \quad (3)$$

where $\alpha, \gamma,$ and β are estimated parameters and *lnQ* is a quantity index equal to $\sum_f \alpha_f \ln(X_f) + \frac{1}{2}\sum_f \sum_g \gamma_{fg} \ln(X_f) \ln(X_g)$.

Welfare Estimation

The concept of consumer welfare that we use in this application is compensating variation (*CV*) and represents the amount of additional income needed to compensate consumers for a change in the supply of a set of goods,

$$CV = Y_1[D(u_0, X_1) - D(u_0, X_0)] - (Y_1 - Y_0). \quad (4)$$

The term in the square brackets is the factor by which total expenditures in the climate change scenario Y_1 would have to be inflated to return consumers to their original level of utility, u_0, after the change in supply from X_0 to X_1. The function $D(u, X)$ is called the *distance function* and represents how consumption would have to change to provide the same level of utility u_0 when the supply vector changes from X_0 to X_1. $D(u, X)$ is a function of the estimated demand system parameters and the supply vectors forecasted under the climate change scenarios. Its functional form is derived from the inverse almost ideal demand system and provided in the supplementary material. The last term in parentheses is included to account for differences in expenditures between climate scenarios. If incomes are expected to be higher or lower under the climate change scenario, expenditures on this set of commodities would change accordingly, and that differential is accounted for when calculating *CV*.

Welfare estimation also proceeds in two stages (Moore and Griffiths 2018). In the first stage, equation (2) is evaluated using the forecasted aggregated quantities for each commodity group to solve for the first stage expenditure shares under each climate scenario. In the second stage, those expenditure shares are used to find expenditures on each commodity group, Y_0 and Y_1. The parameters estimated in the second stage demand systems are then used to solve for *CV* in each commodity group. Finally, *CV* is aggregated across groups to provide total consumer welfare impacts for each year of the simulation.

Harvest Volume and Value Data

Shellfish landings and value data for the US were downloaded from the National Marine Fisheries Service data portal for commercial landings. The models were estimated on annual data from 1950 through 2020 for most species. Some species had missing years in which commercial harvest was negligible that were omitted from estimation. Canadian landings and value data were downloaded from the Department of Fisheries and Oceans for the years 1990 through 2020. All value data were converted to 2020 US dollars for the welfare analysis.

Estimating a Reduced Form Damage Function

Damage functions allow for rapid assessments of the economic impacts from climate change. The relationship between temperature, ocean acidification (pH), and economic impacts in the US and

Canada can be applied to custom scenarios to efficiently estimate damages under different emissions or policy pathways without modeling all intervening physical and behavioral outcomes for each scenario. The inputs to the physical model and outputs from the economic model (figure 1) provide datapoints from which a reduced form damage function can be estimated. The resulting function provides a direct mapping from climate inputs, such as temperature, to annual economic impacts. Although we present welfare estimates for RCP 8.5 and RCP 2.6, only RCP 8.5 impacts are processed for the damage function. The selection of a higher emissions scenario ensures that we evaluate the broadest range of impacts. The simplification embodied by a time-invariant damage function comes at the cost of assuming away path-dependence of economic damages. If certain levels of temperature increases are realized gradually, adaptation measures are likely to reduce the economic impacts relative to a scenario where those changes are realized over a shorter amount of time.

We develop the reduced form damage function by estimating a statistical relationship between the projected climate variables and the consumer welfare impacts in each year of the simulation. Damage functions for the US and Canada are estimated separately. Ordinary least squares (OLS) regression is sufficient to estimate the relationship since all variables of interest are continuous and the estimating equation is linear. We average values from the three CMIP5 Earth system models to generate a single set of potential independent variables. Finally, we compare model fit across several specifications to select a single set of regressors.

Results

The relative changes in maximum catch potential for each type of shellfish forecasted with the DBEM are the primary inputs to the consumer welfare model. Annual changes in consumer welfare are, in turn, used to estimate the reduced form damage functions. We present the results of each modeling step, in sequence, below.

Forecasted Changes in Maximum Catch Potential

Figure 2 shows the forecasted proportional change in harvest of the four most valuable shellfisheries in the US and Canada through 2100 under RCP 2.6 and RCP 8.5. The projected impacts under RCP 2.6 in the US are small and all four harvests are projected to return to within 6% of current levels by the end of the century. Projections under RCP 8.5 are far more pronounced. The shellfish with the highest valued annual harvest, American lobster, shows the largest relative decline with projected harvests falling by 62% by the end of the century. Shrimp and sea scallop harvests are also expected to decline considerably under the severe climate change scenario. However, dungeness crab harvests are expected to increase by more than 40% by 2100. While some of the dungeness crab harvest occurs off the coast of the contiguous US, all of the projected increases occur in Alaskan waters.

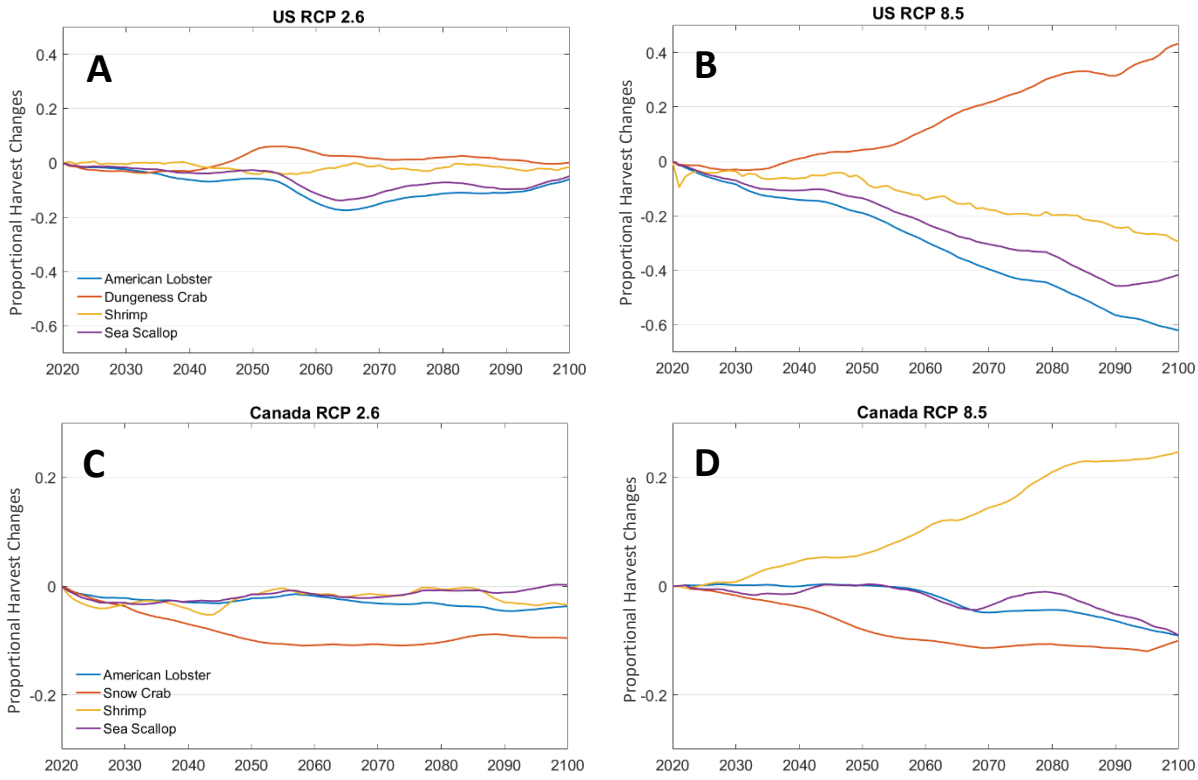

Figure 2. Projected proportional changes in harvest from ocean warming and acidification for the four most valuable shellfisheries in (A) the US under mitigation scenario RCP 2.6, (B) the US under RCP 8.5, (C) Canada under RCP 2.6, and (D) Canada under RCP 8.5.

The projected impacts to Canadian harvests under RCP 2.6 are similarly small with the greatest decline projected for snow crab at nearly 10%. Declines in Canadian harvest under the RCP 8.5 scenario are remarkably similar for snow crab, lobster, and sea scallops - all falling by about 10%. Projections of shrimp harvest, however, rise to 125% of current levels under the severe climate change scenario. Taken together, the US and Canadian harvest projections tell a story of climate-induced range shifts creating winners and losers across different fisheries.

Consumer Welfare Impacts

Demand system estimation results for the US and Canada are reported in the supplementary material. The models perform well and the signs and magnitudes of the estimated coefficients are consistent with prior expectations based on economic theory.

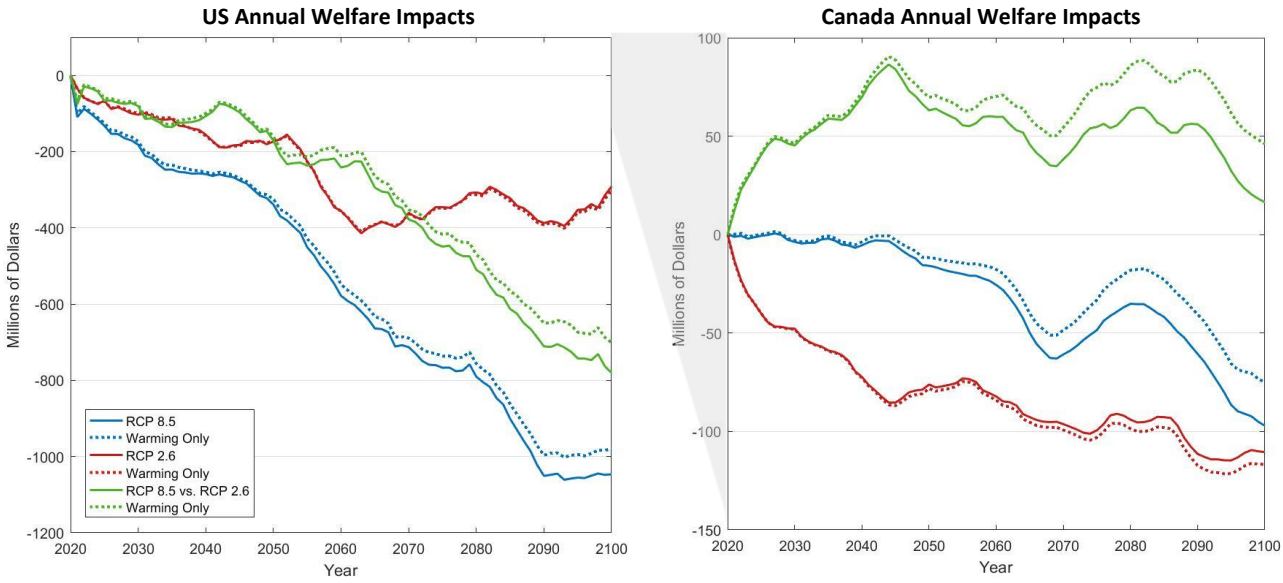

Figure 3. Annual shellfish consumer welfare impacts in the US (left) and Canada (right). Red and blue lines represent impacts under RCP 2.6 and 8.5 compared to current conditions. Green lines represent the impacts of RCP 8.5 relative to an RCP 2.6 alternative. Solid lines indicate total impacts from greenhouse gasses and dashed lines show impacts attributable to warming only.

The projections generated by the DBEM and used in the consumer welfare model allow us to make several revealing comparisons. Figure 3 shows how the impacts compare between scenarios, within each country. In the US, annual impacts exceed one billion dollars per year at the end of the century under the RCP 8.5 scenario and briefly exceed $400 million under RCP 2.6 in the second half of the century. In Canada, consumers experience much smaller welfare impacts, with damages under the RCP 2.6 scenario exceeding those under RCP 8.5. This is primarily due to the favorable conditions for shrimp in the warming Canadian waters under the high climate change scenario. While the current value of the US harvest is about 1.5 times that of Canada's, that 50% difference in baseline value explains only a fraction of the difference in welfare impacts between the countries. The bulk of the difference, which approaches a factor of ten by the end of the century in the RCP 8.5 scenario, is driven instead by changes in habitat suitability. Each plot in Figure 3 contains a third set of results showing welfare impacts of the RCP 8.5 scenario while treating RCP 2.6 as the baseline. Such a comparison could be more useful to decision makers because it compares two alternative futures, rather than comparing future and current conditions. The values of the scenario comparisons are similar, but not necessarily equal to, the vertical distance between the RCP 2.6 and 8.5 welfare values. Notice the value of the scenario comparison for Canadian consumers is above zero indicating that a high climate change future would produce modest net gain in shellfish markets relative to the strict mitigation scenario.

An additional comparison we can perform using the results of the DBEM reveals how much of the consumer welfare impacts are attributable to warming alone and how much are driven by ocean acidification. The distance between the dashed and solid lines of the same color show that ocean acidification in US waters accounts for less than 7% of the damages under RCP 8.5 and 4% under RCP 2.6 by the end of the century. Canadian impacts attributable to acidification account for somewhat larger percentages of the total but are smaller in absolute terms.

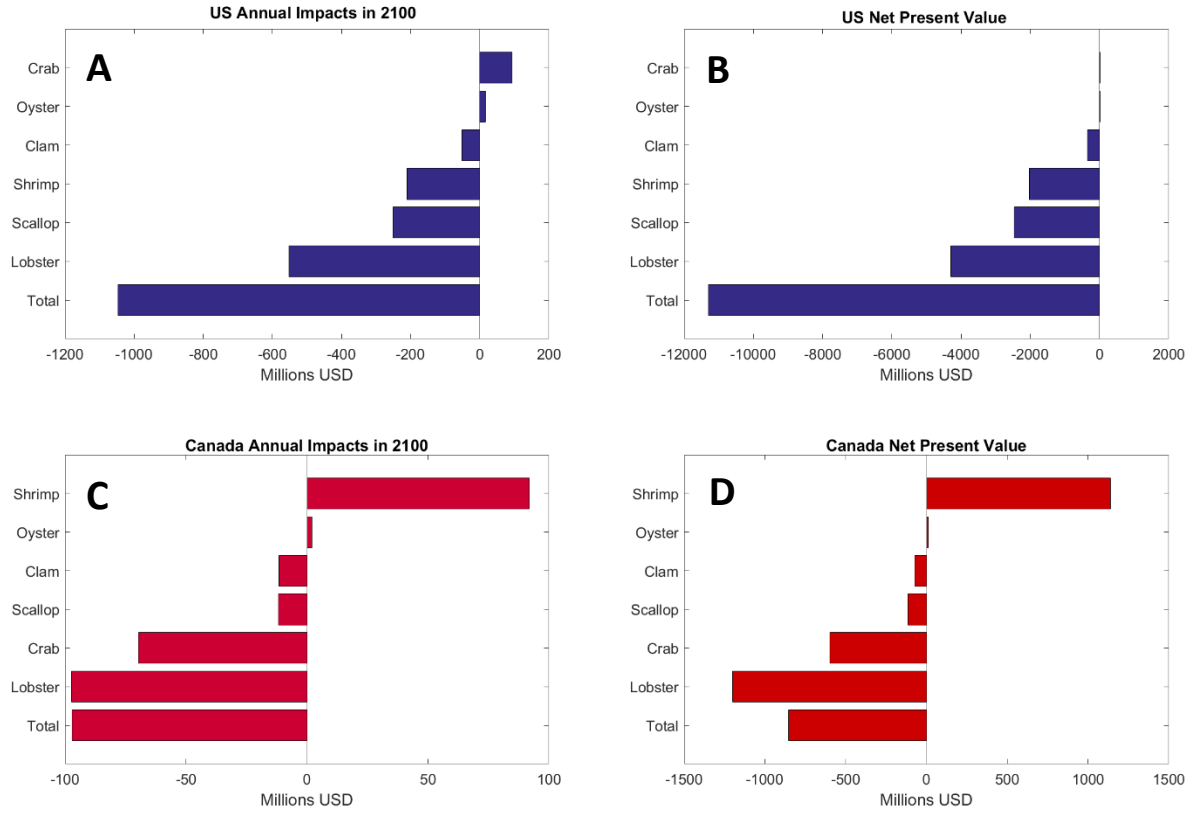

Figure 4. Consumer welfare impacts under the high emissions scenario RCP 8.5 (A) in the US in the year 2100, (B) the net present value of impacts from 2020 to 2100 discounted at 3% per year[3], (C) in Canada in the year 2100, and (D) the net present value of impacts to Canadian consumers through 2100 discounted at 3%.

The panels of Figure 4 combine similar species and aggregate the consumer welfare impacts for each group. Annual impacts in the year 2100 and the net present value (NPV) of impacts projected through the end of the century are presented side by side. The NPV of total impacts is about $11.3 billion in the US and $850 million in Canada. From these figures, it is clear that the modest positive impacts in some US fisheries are far out paced by the negative impacts in others. The positive impacts *to Canadian shrimp harvests, however, compensate* for the largest damages in the lobster market.

The change in global mean temperature is a sufficient explanatory variable for annual welfare impacts and, as Figure 5 shows, a linear functional form captures the relationship between temperature change and economic impacts well in the US and Canada. Our estimation supresses the constant term in both regressions, forcing the damage function to pass through zero and implying no economic impacts when temperature change is zero. The slope coefficient for Canadian damages indicates $20 million in annual damages for every degree Celsius increase. The slope of the damage function for the US is much greater, implying $318 million in annual damages for every degree of warming. Both damage function slope coefficients are statistically significant at the 0.01 level.

[3] Future changes in consumer welfare are often discounted at 3% per year to recognize the rate of time preference for consumption and the historical growth of per capita consumption over time. See OMB Circular A-4 (p. 75) for a discussion https://www.whitehouse.gov/wp-content/uploads/2023/11/CircularA-4.pdf.

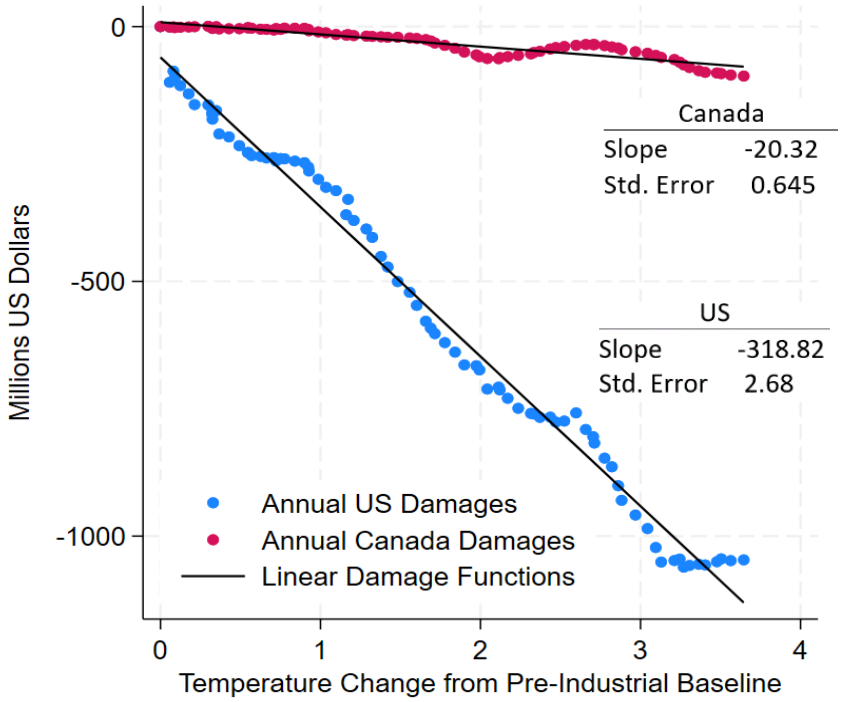

Figure 5. Annual consumer welfare impacts plotted against global mean temperature change and the estimated linear damage functions for the US and Canada.

Discussion and Conclusion

Our simulations of shellfish population dynamics and market responses reveal several interesting results. First, as one might expect, annual economic damages are far greater in the US than they are in Canada. This is due to the size of the shellfish markets in each country and the colder seawater temperatures in Canada that allow some types of shellfish, such as shrimp, to thrive in Canadian waters under the severe climate change scenario. The US experiences a similar increase in the harvest of dungeness crab in the colder Alaskan exclusive economic zone (EEZ), but the volume and value of that fishery is not large enough to offset large losses in other fisheries. These spatial and population dynamics result in Canada experiencing smaller shellfish consumer losses under the severe climate change scenario than it would under the strict mitigation scenario. Finally, the results show that warming will have a much larger impact on habitat suitability and population growth for this set of commercially valuable shellfish than the impacts of ocean acidification. This attribution of thermal versus acidification stress for marine organisms, and the relative importance of each, may be an important consideration for climate mitigation strategies which involve marine geoengineering.

The integrated bioclimatic-economic model that we develop in this paper makes several meaningful contributions to the literature on the marine impacts of climate change. First, very few studies have combined a structural model of population dynamics and a utility theoretic model of social

welfare. It is more common for impact valuation studies to apply a proxy, such as changes in the rate of shell growth (e.g., Cooley and Doney 2009; Moore 2015), rather than develop a spatially explicit model of habitat suitability that is initialized with observational data. Likewise, economic impacts are more often estimated using changes in revenue (e.g., Fernandes et al. 2017) as opposed to a valid concept of social welfare that takes consumer substitution possibilities and real income growth into consideration. Finally, our estimation of reduced form damage functions that will circumvent the need to repeat the integrated assessment modeling for alternative scenarios is a substantial contribution. Given the high confidence in our coefficient estimates and the remarkably linear nature of the damage functions, rapid assessment of these impacts under alternative time paths for global mean temperature will generate informative results.

References

Barten, A. P., and L. J. Bettendorf. 1989. “Price Formation of Fish: An Application of an Inverse Demand System.” *European Economic Review* 33 (8): 1509–25. https://doi.org/10.1016/0014-2921(89)90075-5.

Bednaršek, Nina, Piero Calosi, Richard A. Feely, Richard Ambrose, Maria Byrne, Kit Yu Karen Chan, Sam Dupont, et al. 2021. “Synthesis of Thresholds of Ocean Acidification Impacts on Echinoderms.” *Frontiers in Marine Science* 8. https://www.frontiersin.org/articles/10.3389/fmars.2021.602601.

Berger, Halle. 2022. “The Ocean Acidification Regional Vulnerability Assessment Workshop Report.” https://doi.org/10.25923/7AWD-C445.

Bopp, L, L Resplandy, J C Orr, S C Doney, J P Dunne, M Gehlen, P Halloran, C Heinze, and T Ilyina. 2013. “Multiple Stressors of Ocean Ecosystems in the 21st Century: Projections with CMIP5 Models.” *Biogeosciences* 10: 6225–45. https://doi.org/10.5194/bg-10-6225-2013.

BRANDER, LUKE M., KATRIN REHDANZ, RICHARD S. J. TOL, and PIETER J. H. VAN BEUKERING. 2012. “THE ECONOMIC IMPACT OF OCEAN ACIDIFICATION ON CORAL REEFS.” *Climate Change Economics*, August. https://doi.org/10.1142/S2010007812500029.

Cheung, William W. L., John Dunne, Jorge L. Sarmiento, and Daniel Pauly. 2011. “Integrating Ecophysiology and Plankton Dynamics into Projected Maximum Fisheries Catch Potential under Climate Change in the Northeast Atlantic.” *ICES Journal of Marine Science* 68 (6): 1008–18. https://doi.org/10.1093/icesjms/fsr012.

Cheung, William W L, Vicky W Y Lam, and Daniel Pauly. 2008. “DYNAMIC BIOCLIMATE ENVELOPE MODEL TO PREDICT CLIMATE- INDUCED CHANGES IN DISTRIBUTION OF MARINE FISHES AND INVERTEBRATES.” In *Fisheries Centre Research Reports*, 3rd ed., 16:5–50.

Cheung, William W L, Gabriel Reygondeau, and Thomas L Frölicher. 2016. “Large Benefits to Marine Fisheries of Meeting the 1.5°C Global Warming Target.” *Science* 6319 (354): 1591–94.

Cooley, Sarah R., and Scott C. Doney. 2009. “Anticipating Ocean Acidification’s Economic Consequences for Commercial Fisheries.” *Environmental Research Letters* 4 (2): 024007. https://doi.org/10.1088/1748-9326/4/2/024007.

Deaton, Angus, and John Muellbauer. 1980. “An Almost Ideal Demand System.” *The American Economic Review* 70 (3): 312–26.

Doney, Scott C., D. Shallin Busch, Sarah R. Cooley, and Kristy J. Kroeker. 2020. “The Impacts of Ocean Acidification on Marine Ecosystems and Reliant Human Communities.” *Annual Review of Environment and Resources* 45 (1): 83–112. https://doi.org/10.1146/annurev-environ-012320-083019.

Edgerton, David L. 1997. “Weak Separability and the Estimation of Elasticities in Multistage Demand Systems.” *American Journal of Agricultural Economics* 79 (1): 62–79. https://doi.org/10.2307/1243943.

Ekstrom, Julia A., Lisa Suatoni, Sarah R. Cooley, Linwood H. Pendleton, George G. Waldbusser, Josh E. Cinner, Jessica Ritter, et al. 2015. “Vulnerability and Adaptation of US Shellfisheries to Ocean Acidification.” *Nature Climate Change* 5 (3): 207–14. https://doi.org/10.1038/nclimate2508.

Fernandes, Jose A, Eleni Papathanasopoulou, Caroline Hattam, Ana M Queirós, William W W L Cheung, Andrew Yool, Yuri Artioli, et al. 2017. “Estimating the Ecological, Economic and Social Impacts of Ocean Acidification and Warming on UK Fisheries.” *Fish and Fisheries* 18 (3): 389–411. https://doi.org/10.1111/faf.12183.

Kroeker, Kristy J., Rebecca L. Kordas, Ryan Crim, Iris E. Hendriks, Laura Ramajo, Gerald S. Singh, Carlos M. Duarte, and Jean-Pierre Gattuso. 2013. “Impacts of Ocean Acidification on Marine Organisms: Quantifying Sensitivities and Interaction with Warming.” *Global Change Biology* 19 (6): 1884–96. https://doi.org/10.1111/gcb.12179.

Moore, Chris. 2015. “Welfare Estimates of Avoided Ocean Acidification in the U.S. Mollusk Market.” *Journal of Agricultural and Resource Economics* 40 (1): 50–62.

Moore, Chris, and Jasmine Fuller. 2022. “Economic Impacts of Ocean Acidification: A Meta-Analysis.” *Marine Resource Economics* 37 (2): 201–19. https://doi.org/10.1086/718986.

Moore, Chris, and Charles Griffiths. 2018. “Welfare Analysis in a Two-Stage Inverse Demand Model: An Application to Harvest Changes in the Chesapeake Bay.” *Empirical Economics* 55 (3): 1181–1206. https://doi.org/10.1007/s00181-017-1309-3.

Moore, Chris, James W. Morley, Brian Morrison, Michael Kolian, Eric Horsch, Thomas Frölicher, Malin L. Pinsky, and Roger Griffis. 2021. “Estimating the Economic Impacts of Climate Change on 16 Major Us Fisheries.” *Climate Change Economics* 12 (01): 2150002. https://doi.org/10.1142/S2010007821500020.

Narita, Daiju, and Katrin Rehdanz. 2017. “Economic Impact of Ocean Acidification on Shellfish Production in Europe.” *Journal of Environmental Planning and Management* 60 (3): 500–518. https://doi.org/10.1080/09640568.2016.1162705.

Narita, Daiju, Katrin Rehdanz, and Richard S. J. Tol. 2012. “Economic Costs of Ocean Acidification: A Look into the Impacts on Global Shellfish Production.” *Climatic Change* 113 (3): 1049–63. https://doi.org/10.1007/s10584-011-0383-3.

Palomares, Maria Lourdes D, William W L Cheung, Vicky W Y Lam, and Daniel Pauly. 2016. “THE DISTRIBUTION OF EXPLOITED MARINE BIODIVERSITY.” In *Global Atlas of Marine Fisheries: A Critical Appraisal of Catches and Ecosystem Impacts*, 46–58. Island Press.

Park, Hoanjae, Walter N. Thurman, and Easley J.e. 2004. “Modeling Inverse Demands for Fish: Empirical Welfare Measurement in Gulf and South Atlantic Fisheries.” *Marine Resource Economics* 19 (3): 333–51. https://doi.org/10.1086/mre.19.3.42629438.

Pauly, Daniel. 1980. “On the Interrelationships between Natural Mortality, Growth Parameters, and Mean Environmental Temperature in 175 Fish Stocks.” *ICES Journal of Marine Science* 39 (2): 175–92. https://doi.org/10.1093/icesjms/39.2.175.

Pauly, Daniel, and William W. L. Cheung. 2018. “Sound Physiological Knowledge and Principles in Modeling Shrinking of Fishes under Climate Change.” *Global Change Biology* 24 (1): e15–26. https://doi.org/10.1111/gcb.13831.

Pauly, Daniel, and Dirk Zeller. 2015. “Sea Around Us Concepts, Design and Data.” seaaroundus.org.

Pinsky, Malin L., Gabriel Reygondeau, Richard Caddell, Juliano Palacios-Abrantes, Jessica Spijkers, and William W. L. Cheung. 2018. “Preparing Ocean Governance for Species on the Move.” *Science* 360 (6394): 1189–91. https://doi.org/10.1126/science.aat2360.

Rennert, Kevin, Frank Errickson, Brian C. Prest, Lisa Rennels, Richard G. Newell, William Pizer, Cora Kingdon, et al. 2022. “Comprehensive Evidence Implies a Higher Social Cost of CO2.” *Nature* 610 (7933): 687–92. https://doi.org/10.1038/s41586-022-05224-9.

Speers, Ann E., Elena Y. Besedin, James E. Palardy, and Chris Moore. 2016. “Impacts of Climate Change and Ocean Acidification on Coral Reef Fisheries: An Integrated Ecological–Economic Model.” *Ecological Economics* 128 (August): 33–43. https://doi.org/10.1016/j.ecolecon.2016.04.012.

Tai, Travis C., Christopher D.G. Harley, and William W.L. Cheung. 2018. “Comparing Model Parameterizations of the Biophysical Impacts of Ocean Acidification to Identify Limitations and Uncertainties.” *Ecological Modelling* 385 (October): 1–11. https://doi.org/10.1016/j.ecolmodel.2018.07.007.

Tai, Travis C., U. Rashid Sumaila, and William W. L. Cheung. 2021. “Ocean Acidification Amplifies Multi-Stressor Impacts on Global Marine Invertebrate Fisheries.” *Frontiers in Marine Science* 8. https://www.frontiersin.org/articles/10.3389/fmars.2021.596644.

U.S. EPA. 2022. “Supplementary Material for the Regulatory Impact Analysis for the Supplemental Proposed Rulemaking, ‘Standards of Performance for New, Reconstructed, and Modified Sources and Emissions Guidelines for Existing Sources: Oil and Natural Gas Sector Climate Review’: EPA External Review Draft of Report on the Social Cost of Greenhouse Gases: Estimates Incorporating Recent Scientific Advances.” EPA-HQ-OAR-2021-0317.

Walters, Carl J., and Steven J. D. Martell. 2004. *Fisheries Ecology and Management*. Princeton University Press.

Supplementary Material

Methods

1. Shellfish types included in consumer welfare model

   Tai, Sumaila, and Cheung (2021) report maximum catch potential (MCP) projections through the year 2100 for 210 commercially harvested marine invertebrates. To estimate consumer welfare impacts from those projections, the economic model requires consistently reported historical data on the amount of each shellfish type harvested and the annual average dockside price.

   In the US, the NOAA Commercial Landings Database provides sufficient data for 18 types of shellfish:

   1. Quahog
   2. Soft clam
   3. Geoduck
   4. Surf clam
   5. Blue crab
   6. King crab
   7. Dungeness crab
   8. Tanner crab
   9. American lobster
   10. Caribbean spiny lobster
   11. Eastern
   12. Pacific
   13. Bay scallop
   14. Sea scallop
   15. Weathervane scallop
   16. Brown shrimp
   17. Pink shrimp
   18. White shrimp

   The Canadian Department of Fisheries and Oceans provides sufficient data for seven types of shellfish, some of which are aggregate groups of multiple types:

   1. Dungeness crab
   2. Snow crab
   3. Lobster
   4. Shrimp
   5. Clam
   6. Oyster
   7. Scallop

2. Dynamic bioclimate envelope model

2.1 Modelling individual growth

The von Bertalanffy growth model (Equation 1) assumes body weight is scaled with the exponent $d < 1$ while it is scaled linearly with catabolism. Values of d typically fall between 0.5 and 0.95 across invertebrate species, and we assume $d = 0.7$ for our model simulations. Other values of d have been tested in previous studies; larger values resulted in much higher sensitivity to environmental stressors, while smaller values resulted in a minimal decrease in sensitivity (Pauly and Cheung, 2018; Tai et al., 2018).

We use parameter values from SeaLifeBase (www.sealifebase.ca) (Palomares and Pauly, 2017) for maximum body length, l_∞, and growth rate, K, from the von Bertalanffy growth equation, $l_t = l_\infty\left(1 - e^{-K(t-t_0)}\right)$, where l is the length, t is the age in years, and t_0 is the hypothetical age at size zero (Table S.1) (von Bertalanffy, 1957). Maximum body weight, W_∞, is calculated using the length-weight conversion equation, $W = a \cdot l^b$, where a and b are coefficients also taken from SeaLifeBase (Table S.1). Growth rate, K, is related to catabolic coefficient k:

$$K = k(1 - d). \quad \text{(S.1)}$$

Anabolic H and catabolic k coefficients are equal to:

$$H_{i,t} = g_i \cdot [O_2]_{i,t} \cdot e^{-j_1/T_{i,t}} \qquad \text{(S.2)}$$

and

$$k_{i,t} = h_i \cdot [H^+]_{i,t} \cdot e^{-j_2/T_{i,t}} \qquad \text{(S.3)}$$

where $e^{-j/T}$ represents the Arrhenius equation to model the change in chemical reactions as a function of temperature T in degrees Kelvin. The parameters j are equal to E_a/R where E_a is the activation energy and R is the Boltzmann constant, respectively; activation energies are estimated to be 0.388 eV and 0.689 eV, based on Cheung *et al.* (2011), resulting in a j_1 and j_2 of 4500K and 8000K, respectively. Coefficients g_i and h_i are fixed parameters throughout the simulation and estimated by rearranging Equations S.2 and S.3, and substituting rearranged Equations 1 and S.1 and for H and k:

$$g_i = \frac{W_{\infty,0}^{(1-d)} \cdot k_0}{[O_2]_{0,i} \cdot e^{-j_1/T_0}} \qquad \text{(S.4)}$$

and

$$h_i = \frac{K_0/(1-d)}{[H^+]_{0,i} \cdot e^{-j_2/T_0}}, \qquad \text{(S.5)}$$

given initial values of maximum body size $W_{\infty,0}$ and von Bertalanffy growth parameter K_0, and initial environmental conditions of temperature, oxygen concentration, and hydrogen concentration.

We measured impacts of changes in environmental conditions on growth by estimating new $H_{i,t}$ and $k_{i,t}$ coefficients using Equations S.2 and S.3. Equation 1 can be rearranged to solve for a new maximum body size W_∞ using new values of $H_{i,t}$ and $k_{i,t}$, when the growth rate ($dB/dt = 0$):

$$W_{\infty,t}^{(1-d)} = \frac{H_{i,t}}{k_{i,t}} \quad \text{(S.6)}$$

while Equation S.1 can be used to calculate a new growth parameter K.

Changes in mean body size were simulated using a size transition matrix, X, to model the probabilities of an individual growing from one length class to other size classes in one time-step (year) and each grid cell a species was predicted to occur (Cheung et al., 2008b; Quinn II and Deriso, 1999):

$$X_{i,t,l',l} = \frac{\theta_{y,i,t,l',l}}{\sum_l \theta_{y,i,t,l',l}} \quad \text{(S.7)}$$

and

$$\theta_{y,i,t,l',l} = e^{\left[-\frac{\left(l-\left[l_{\infty,i,t}\left(1-e^{-K_{i,t}}\right)+l'\cdot e^{-K_{i,t}}\right]\right)^2}{2\sigma^2}\right]} \text{(S.8)}$$

where l and l' are the length of a particular size class and the adjacent length size classes, l_∞ is the asymptotic length, y is the age of an individual, and K is the von Bertlanffy growth parameter. Variation in growth, σ, assumed to have a coefficient of variation of 20% and is independent of length and age (Cheung et al., 2008b). Our model applies this general size transition model and makes no assumptions of species-specific growth stages (e.g. moulting) or sex.

Mean body size (g), $\overline{W}$, is calculated:

$$\overline{W}_{i,t} = \frac{\sum_y \sum_l W_l \cdot X_{i,t,l',l} \cdot S_{i,t,y-1,l} \cdot e^{-M_{i,t}}}{\sum_y \sum_l X_{i,t,l',l} \cdot S_{i,t,y-1,l} \cdot e^{-M_{i,t}}} \quad \text{(S.9)}$$

where S is a relative distribution length-age frequency matrix from age class t at size class l, and initial relative distribution at age 0 (when $y = 1$) across length classes was assumed to be $S_{i,t,0,l} = \left[1 \;\; 0 \;\; 0 \;\; \cdots \;\; 0_{l_{\infty,i,t}}\right]$. Parameter M is the population natural mortality, calculated from maximum body size W_∞, von Bertalanffy growth parameter K, and temperature $T_{Celsius}$ (in degrees Celsius) using a model developed by (Pauly, 1980):

$$M_{i,t} = -0.4851 - 0.0824\log\left(W_{\infty,i,t}\right) + 0.6757\log\left(K_{i,t}\right) + 0.4687\log\left(T_{Celsius,i,t}\right) \quad \text{(S.10)}$$

Spawning biomass is estimated using the size transition matrix, X, and the mean weight of each size class for size classes greater than the size at maturity, l_{mat} (Pauly, 1984):

$$l_{mat,i,t} = l_{\infty,i,t}(0.714)^{1/(1-d)} \quad \text{(S.11)}$$

Length at maturity is determined for each cell based on the maximum body size l_∞ as determined by Equation 1 and the length-weight conversion equation.

2.2. Modelling population biomass

Biomass (B) can converted to relative abundance (A) using mean weight ($\overline{W}$) with the formula $A_{i,t} = B_{i,t}/\overline{W}_{i,t}$. Average mortality, $\overline{M}$, for each cell was weighted by size class specific mortality rates tested in this study. Grid cells are assumed to be at carrying capacity from the start of the simulation, and carrying capacity changes as a function of habitat suitability, P, and primary production, PP, from initial conditions ($t = 0$) to the current timestep, t, such that:

$$C_{i,t} = C_{i,0} \cdot \frac{P_{i,t}}{P_{i,0}} \cdot \frac{PP_{i,t}}{PP_{i,0}} \quad \text{(S.12)}$$

Habitat suitability is dependent on five environmental factors in combination with species specific traits, such that:

$$P_i = P(T_i, TPP) \cdot P(Bathy_i, MinD, MaxD) \cdot P\left(Habitat_{i,j}, HAssoc\right) \cdot P(Salinity_i, SAssoc) \cdot P(Ice_i, IceP) \quad \text{(S.13)}$$

Habitat suitability is determined by: T is temperature (Kelvin) and *TPP* is the species' temperature preference profile; *Bathy* is the bathymetry and *MinD* and *MaxD* is the minimum and maximum depth of the species range; $Habitat_{i,j}$ is the proportion of total area of a cell with a specific habitat j (e.g. inshore, offshore, coral, estuarine, etc.); *Salinity* is the salinity class of the cell based on Thalassic series—metahaline (> 40 ppt), mixoeuhaline (> 29 ppt), polyhaline (> 18 ppt), mesophaline (> 5 ppt), oligohaline (> 0 ppt)—and *SAssoc* is the association of the species with each salinity class; and Ice_i is the sea ice % area coverage in a cell and *IceP* is the ice-dependency of the species.

The *TPP* was estimated using the initial predicted relative abundance (described above) overlaid with the inputs of earth system models of initial environmental conditions. The relative weight for each temperature class z of the temperature preference profile was calculated as $TPP_z = R_z/\sum R_z$, where R_z is the relative abundance in each temperature class.

A fuzzy logic model was used to model the movement between neighbouring cells based on differences in habitat suitability (Cheung et al., 2008b). Emigration into a cell is favoured if habitat suitability is higher than surrounding cells, and immigration out of a cell is favoured if habitat suitability is lower than surrounding cells.

We estimated larval production as 30% of spawning population biomass for each cell i, while larval mortality was 0.85 day^{-1} and settlement rate was 0.15 day^{-1}—these values were chosen based on the sensitivity testing of these parameters (Cheung et al., 2008b).

Larval dispersal is modelled using an advection-diffusion (Sibert et al., 1999) and a larval duration model based on temperature (O'Connor et al., 2007), such that abundance $A_{i,t}$ in each cell is numerically solved for using the equation:

$$\frac{\partial A_{i,t}}{\partial t} = \frac{\partial}{\partial x}\left(D_{i,t}\frac{\partial A_{i,t}}{\partial x}\right) + \frac{\partial}{\partial y}\left(D_{i,t}\frac{\partial A_{i,t}}{\partial y}\right) - \frac{\partial}{\partial x}\left(u \cdot A_{i,t}\right) - \frac{\partial}{\partial y}\left(v \cdot A_{i,t}\right) - \lambda \cdot A_{i,t} \qquad \text{(S.14)}$$

while adult dispersal is similarly modelled,

$$\frac{\partial A_{i,t}}{\partial t} = \frac{\partial}{\partial x}\left(D_{i,t}\frac{\partial A_{i,t}}{\partial x}\right) + \frac{\partial}{\partial y}\left(D_{i,t}\frac{\partial A_{i,t}}{\partial y}\right) \qquad \text{(S.15)}$$

Advection was modelled for larval dispersal using parameters *u* and *v* for horizontal (east-west) and vertical (north-south) directions for surface current velocity ($m^2 \cdot s^{-1}$), respectively, between neighbouring cells *x* and *y* in the east-west and north-south direction, respectively. Instantaneous rate of larval mortality, M_L, and settlement, S_L was integrated into equation (16), where $\lambda = 1 - e^{-(M_L + S_L)}$. The coefficient $D_{i,t}$ is the diffusion parameter:

$$D_{i,t} = \frac{D_{i,0}m}{1+e^{\left(\tau \cdot P_{i,t} \cdot \rho_{i,t}\right)}} \qquad \text{(S.16)}$$

and

$$\rho_{i,t} = 1 - \frac{\emptyset_{i,t}}{\left(C_{i,t}/\overline{W}_{i,t}\right)} \qquad \text{(S.17)}$$

where $D_{i,0}$ is the initial diffusion coefficient and a function of the spatial grid size (*GR*): $D_{i,0} = (1.1 \cdot 10^4) \cdot GR \cdot 1.33$. Parameters *m* and τ—both set at 2 in the model—determine the curvature of the functional relationship between *D*, *P*, and ρ (Cheung et al., 2008b). Parameter $\rho_{i,t}$ represents density-dependent factors and a function of population density $\emptyset_{i,t}$ (number of individuals), carrying capacity ($C_{i,t}$), and mean body weight ($\overline{W}_{i,t}$) in each cell *i*.

2.3 Modelling effects on survival

OA effects can be modelled as relative changes in survival rate for all life stages in Table 2. In other words, percent changes in acidity (*i.e.* hydrogen ion concentration) from baseline initial conditions results in a percent change in baseline survival rate. We use a model structure similar to that of previous work we have done (Tai et al., 2018):

$$Surv_t = Surv_{init} \cdot \left[1 + \left(p \cdot \left(\frac{[H^+]_t}{[H^+]_{init}} - 1\right)^w\right)\right] \qquad \text{(S.18).}$$

Surv is the survival rate per year and used here as an example but can be applied to other life histories affected by OA (e.g. growth, reproduction). Survival rate in year *t* is derived from the initial (*init*) survival rate and the relative change in $[H^+]$ between year *t* and initial $[H^+]$ conditions. Note that in our previous model, *p* represents the point value of the percent change effect size with a doubling of $[H^+]$. This model utilizes single point effect size estimates that have no underlying assumed relationship between acidity and survival. In our model, we used an exponent value, *w*, equal to 1, which assumes a linear relationship (Tai et al., 2018).

We used parameters derived from previous experimental studies, where they observed a ~15% increase in mortality (Kroeker et al., 2013) from a doubling of hydrogen ion concentration.

All statistical analyses and figures were generated using the programming software R v4.0.3 (R Core Team, 2020).

3. Consumer Demand and Welfare Model

3.1 Derivation of the distance function from the Inverse Almost Ideal Demand System

The logarithmic distance function analogous to Deaton and Muellbauer's (1980) Almost Ideal Demand System model as specified by Moschini and Vissa (1992) is

$$ln[D(U,\boldsymbol{X})] = a(\boldsymbol{X}) - U \cdot b(\boldsymbol{X}) \tag{S.19}$$

where

$$a(\boldsymbol{X}) = \alpha_0 + \sum_i \alpha_i \ln(X_i) + (\tfrac{1}{2}) \sum_i \sum_j \gamma_{ij} \ln(X_i) \ln(X_j) \tag{S.20}$$

$$b(\boldsymbol{X}) = \beta_0 \Pi_i X_i^{\beta_i} \tag{S.21}$$

$\mathbf{X}$ is the quantity vector, $\mathbf{X}=\{X_1,\ldots,X_i,\ldots,X_N\}$, and U is utility. The distance function measures how this quantity vector must be scaled in order to achieve the utility level, U. The following restrictions ensure that $D(U,\mathbf{X})$ is homogenous of degree one

$$\sum_i \alpha_i = 1 \qquad \sum_i \gamma_{ij} = \sum_j \gamma_{ij} = 0 \qquad \sum_i \beta_i = 0 \qquad \gamma_{ij} = \gamma_{ji}$$

If we evaluate the quantity vector, $\mathbf{X}$ at its optimum, $\mathbf{X}^*$ for utility level U, then $D(U,\mathbf{X}^*)=1$ and $\ln[D(U,\mathbf{X}^*)]=0$. This implies that direct utility at the optimum is

$$U(\boldsymbol{X}^*) = a(\boldsymbol{X})/b(\boldsymbol{X}). \tag{S.22}$$

One property of the distance function is that the differentiation with respect to the quantity for a given sector, i, gives the compensated (Hicksian) inverse demand function of prices in that sector, P_i, normalized by expenditure, Y, as a function of utility and quantity supplied (Deaton 1979),

$$\frac{\partial D(U,\boldsymbol{X})}{\partial X_i} = H_i(U,\boldsymbol{X}) = \frac{P_i(U,\boldsymbol{X})}{Y}. \tag{S.23}$$

Substituting in direct utility, equation (A.4), gives the uncompensated (Marshallian) inverse demand of prices for that sector normalized by expenditure as a function of quantity,

$$M_i(\boldsymbol{X}) = \frac{P_i(\boldsymbol{X})}{Y}. \tag{S.24}$$

The compensated (Hicksian, denoted by the superscript h) inverse budget share in terms of utility and quantities, W^h_i, for sector i evaluated at $\mathbf{X}^*$ so that $D(U,\mathbf{X}^*)=1$ is

$$\frac{\partial \ln[D(U,\boldsymbol{X})]}{\partial \ln[X_i]} = \frac{\partial D(U,\boldsymbol{X})}{\partial X_i} \cdot \frac{X_i}{D(U,\boldsymbol{X})} = \frac{P_i(U,\boldsymbol{X})}{Y} \cdot X_i = W_i^h \tag{S.25}$$

3.2 Demand system estimation results

First and second stages of the consumer demand systems are estimated via seemingly unrelated regression using the *nlsur* command in Stata. The first stage groups and second stage commodities are numbered below for convenience. Parameter estimates for the inverse almost ideal demand model and resulting flexibility estimates will use this numbering convention. The last group and commodities within each group are omitted from the demand system estimation and parameter estimates are backed out to impose the adding up and homogeneity restrictions. The matrix of γ estimates is symmetric so only the lower triangle of that matrix is presented in the tables below (see Moschini and Vissa (1992), Deaton and Muellbauer (1980), and Moore and Griffiths (2018) for details).

The coefficient estimates themselves do not have intuitive interpretations that would provide prior expectations on sign or magnitude based on economic theory. However, the coefficients can be used to calculate the implied own-quantity and scale flexibilities. We use the full estimated covariance matrix to perform a Krinsky-Robb simulation on the implied own-quantity and scale flexibilities for the first stage only. All flexibilities are expected to be negative with magnitudes not much greater than one in absolute value. Mean-to-variance ratios greater than 2 typically reflect quantities that are precisely estimated, akin to t-statistics.

3.2.1 United States Demand System Results

First Stage Groups

1. Clam
2. Crab
3. Lobster
4. Oyster
5. Scallop
6. Shrimp

Second Stage Commodities

Clam

1. Quahog
2. Soft clam
3. Geoduck
4. Surf clam

Crab

1. Blue crab
2. King crab
3. Dungeness crab
4. Tanner crab

Lobster

1. American lobster
2. Caribbean spiny lobster

Oyster

1. Eastern
2. Pacific

Scallop

1. Bay scallop
2. Sea scallop
3. Weathervane scallop

Shrimp

1. Brown
2. Pink
3. White

Table S.2 First stage inverse demand results

	α_1	α_2	α_3	α_4	α_5	β_1	β_2	β_3	β_4	β_5
Estimate	0.240	-0.425	-0.763	0.837	-2.101	0.012	-0.030	-0.057	0.034	-0.135
Standard Error	0.141	0.290	0.224	0.248	0.123	0.008	0.016	0.013	0.014	0.007

	γ_{11}	γ_{12}	γ_{13}	γ_{14}	γ_{15}	γ_{22}	γ_{23}	γ_{24}	γ_{25}	γ_{33}	γ_{34}	γ_{35}	γ_{44}	γ_{45}	γ_{55}
Estimate	0.026	-0.003	-0.035	0.002	-0.050	0.160	0.056	-0.086	0.101	0.156	-0.044	0.189	0.103	-0.108	0.526
Standard Error	0.007	0.011	0.010	0.007	0.027	0.026	0.020	0.017	0.054	0.035	0.020	0.041	0.020	0.046	0.048

Table S.3 First stage flexibilities

	Own-Quantity	Mean/StDev	Scale	Mean/StDev
Clam	-0.737	-10.98	-1.143	-11.20
Crab	-0.352	-5.09	-0.862	-11.29
Lobster	-0.427	-6.93	-0.612	-6.97
Oyster	-0.342	-3.13	-1.326	-9.84
Scallop	0.063	0.86	0.273	4.44
Shrimp	-0.395	-4.20	-1.506	-26.57

Table S.4 Second stage results

	α_1	α_2	α_3	β_1	β_2	β_3	γ_{11}	γ_{12}	γ_{13}	γ_{22}	γ_{23}	γ_{33}
Clam												
Estimate	0.880	0.974	0.492	0.020	0.049	0.023	0.051	0.026	-0.003	0.068	-0.008	0.038
Std Error	0.216	0.168	0.173	0.014	0.010	0.011	0.015	0.009	0.008	0.013	0.006	0.008

Crab												
Estimate	1.522	-1.196	0.802	0.079	-0.090	0.031	0.246	-0.209	0.012	0.284	-0.110	0.119
Std Error	0.288	0.350	0.245	0.016	0.019	0.014	0.049	0.053	0.018	0.071	0.027	0.017
Lobster												
Estimate	1.23			0.32			-0.28					
Std Error	0.10			0.04			0.04					
Oyster												
Estimate	0.59			0.67			-0.50					
Std Error	0.29			0.05			0.05					
Scallop												
Estimate	0.51	0.14		-0.04	0.03		0.03	-0.04		0.06		
Std Error	0.24	0.30		0.02	0.01		0.01	0.01		0.01		
Shrimp												
Estimate	1.33	0.99		0.05	0.04		0.28	-0.01		0.11		
Std Error	0.45	0.49		0.03	0.03		0.05	0.02		0.03		

3.2.2 Canada Demand System Results

Canada's reporting of harvest and dockside price data is not as detailed as the United States'. As a result, there are only two groups in the first stage demand system: crustaceans and mollusks. The second stage numbering of the commodities in each group are listed below.

Crustaceans

1. Dungeness crab
2. Snow crab
3. Lobster
4. Shrimp

Mollusks

1. Clam
2. Oyster
3. Scallop

Table S.5 Crustacean results

	α_1	α_2	α_3	β_1	β_2	β_3	γ_{11}	γ_{12}	γ_{13}	γ_{22}	γ_{23}	γ_{33}
Estimate	0.009	-2.022	1.618	-0.002	-0.123	0.059	0.010	0.013	-0.007	0.495	-0.242	0.180
Std Error	0.120	0.614	0.544	0.007	0.033	0.029	0.007	0.021	0.008	0.168	0.099	0.064

Table S.6 Mollusk results

	α_1	α_2	β_1	β_2	γ_{11}	γ_{12}	γ_{22}
Estimate	0.476	0.084	0.000	-0.002	0.155	-0.008	0.029
Std Error	1.177	0.276	0.065	0.015	0.027	0.007	0.005

Table S.7 Second stage flexibilities

Mollusks	**Own-Quantity**	**Mean/StDev**	**Scale**	**Mean/StDev**
Dungeness	-0.716	-2.873	-0.925	-4.308
Snow Crab	-0.189	-0.891	-0.548	-4.600
Lobster	-0.856	-13.286	-1.120	-19.172
Shrimp	-0.510	-3.202	-1.332	-10.078
Crustaceans	**Own-Quantity**	**Mean/StDev**	**Scale**	**Mean/StDev**
Clam	-0.780	-2.889	-0.996	-5.950
Oyster	-0.196	-0.713	-0.936	-1.778
Scallop	-0.856	-4.177	-1.006	-9.126

References

Bopp, L., Resplandy, L., Orr, J. C., Doney, S. C., Dunne, J. P., Gehlen, M., et al. (2013). Multiple stressors of ocean ecosystems in the 21st century: projections with CMIP5 models. *Biogeosciences* 10, 6225–6245. doi:10.5194/bg-10-6225-2013.

Cheung, W. W., Close, C., Lam, V., Watson, R., and Pauly, D. (2008a). Application of macroecological theory to predict effects of climate change on global fisheries potential. *Mar. Ecol. Prog. Ser.* 365, 187–197. doi:10.3354/meps07414.

Cheung, W. W. L., Dunne, J., Sarmiento, J. L., and Pauly, D. (2011). Integrating ecophysiology and plankton dynamics into projected maximum fisheries catch potential under climate change in the Northeast Atlantic. *ICES J. Mar. Sci.* 68, 1008–1018. doi:10.1093/icesjms/fsr012.

Cheung, W. W. L., Lam, V. W. Y., and Pauly, D. (2008b). Modelling Present and Climate-Shifted Distribution of Marine Fishes and Invertebrates. *Fish. Cent. Res. Reports* 16, 76.

Cheung, W. W. L., Reygondeau, G., and Frölicher, T. L. (2016). Large benefits to marine fisheries of meeting the 1.5°C global warming target. *Science (80-.).* 6319, 1591–1594.

Deaton A., Muellbauer J. (1980). An almost ideal demand system. *The American Economic Review* 70:312-326

Dunne, J. P., John, J. G., Shevliakova, S., Stouffer, R. J., Krasting, J. P., Malyshev, S. L., et al. (2013). GFDL's ESM2 global coupled climate-carbon earth system models. Part II: Carbon system formulation and baseline simulation characteristics. *Am. Meteorol. Soc.* 26, 2247–2267. doi:10.1175/JCLI-D-12-00150.1.

Hilborn, R., and Walters, C. J. (1992). *Quantitative Fisheries Stock Assessment*. Boston, MA: Springer US doi:10.1007/978-1-4615-3598-0.

Kroeker, K. J., Kordas, R. L., Crim, R., Hendriks, I. E., Ramajo, L., Singh, G. S., et al. (2013). Impacts of ocean acidification on marine organisms: Quantifying sensitivities and interaction with warming. *Glob. Chang. Biol.* 19, 1884–1896. doi:10.1111/gcb.12179.

Moschini G., Vissa A. (1992). A linear inverse demand system. *Journal of Agricultural and Resource Economics*:294-302

O'Connor, M. I., Bruno, J. F., Gaines, S. D., Halpern, B. S., Lester, S. E., Kinlan, B. P., et al. (2007). Temperature control of larval dispersal and the implications for marine ecology, evolution, and conservation. *Proc. Natl. Acad. Sci. U. S. A.* 104, 1266–71. doi:10.1073/pnas.0603422104.

Palomares, M. L. D., and Pauly, D. (2017). SeaLifeBase. *World Wide Web Electron. Publ.*, version (06/2017). Available at: www.sealifebase.org [Accessed January 1, 2017].

Pauly, D. (1980). On the interrelationships between natural mortality, growth parameters, and mean environmental temperature in 175 fish stocks. *ICES J. Mar. Sci.* 39, 175–192.

Pauly, D. (1984). A mechanism for the juvenile-to-adult transition in fishes. *ICES J. Mar. Sci.* 41, 280–284. doi:10.1093/icesjms/41.3.280.

Pauly, D., and Cheung, W. W. L. (2017). Sound physiological knowledge and principles in modeling shrinking of fishes under climate change. *Glob. Chang. Biol.*, 1–12. doi:10.1111/gcb.13831.

Pauly, D., and Cheung, W. W. L. (2018). On confusing cause and effect in the oxygen limitation of fish. *Glob. Chang. Biol.* 24, e743–e744. doi:10.1111/gcb.14383.

Pauly, D., and Zeller, D. (2015). Sea Around Us Concepts, Design and Data (seaaroundus.org).

Quinn II, T. J., and Deriso, R. B. (1999). *Quantitative Fish Dynamics*. doi:10.1007/s13398-014-0173-7.2.

R Core Team (2020). R: A language and environment for statistical computing. Available at: https://www.r-project.org/.

Sibert, J. R., Hampton, J., Fournier, D. A., and Bills, P. J. (1999). An advection-diffusion-reaction model for the estimation of fish movement par ... *Can. J. Fish. Aquat. Sci.* 56, 925–938.

Tai, T. C., Harley, C. D. G., and Cheung, W. W. L. (2018). Comparing model parameterizations of the biophysical impacts of ocean acidification to identify limitations and uncertainties. *Ecol. Modell.* 385, 1–11. doi:10.1016/j.ecolmodel.2018.07.007.

van Vuuren, D. P., Edmonds, J., Kainuma, M., Riahi, K., Thomson, A., Hibbard, K., et al. (2011). The representative concentration pathways: An overview. *Clim. Change* 109, 5–31. doi:10.1007/s10584-011-0148-z.

von Bertalanffy, L. (1957). Quantitative laws in metabolism and growth. *Q. Rev. Biol.* 32.

Walters, C., and Martell, S. (2004). *Fisheries Ecology and Management*. 1st editio. Princeton University Press.